Bioorganic Chemistry 86 (2019) 166–175

Contents lists available at ScienceDirect

Bioorganic Chemistry

journal homepage: www.elsevier.com/locate/bioorg

Design, synthesis and biological evaluation of N-(4-(2-(6,7-dimethoxy-3,4-dihydroisoquinolin-2(1H)-yl)ethyl)phenyl)-4-oxo-3,4-dihydrophthalazine-1-carboxamide derivatives as novel P-glycoprotein inhibitors reversing multidrug resistance

Qianqian Qiu[a,1], Jiaqi Zhou[b,1], Wei Shi[b], Mutta Kairuki[b], Wenglong Huang[b,c,*], Hai Qian[b,c,*]

[a] School of Pharmacy, Jiangsu Provincial Key Laboratory of Coastal Wetland Bioresources and Environmental Protection, Yancheng Teachers' University, Yancheng 224007, PR China
[b] Center of Drug Discovery, State Key Laboratory of Natural Medicines, China Pharmaceutical University, 24 Tongjiaxiang, Nanjing 210009, PR China
[c] Jiangsu Key Laboratory of Drug Discovery for Metabolic Disease, China Pharmaceutical University, 24 Tongjiaxiang, Nanjing 210009, PR China

ARTICLE INFO

Keywords:
Multidrug resistance
P-glycoprotein inhibitors
Doxorubicin

ABSTRACT

The overexpression of P-glycoprotein plays an important role in the process of multidrug resistance (MDR). P-gp inhibitors are one of the effective strategies to reverse tumor MDR. Novel P-gp inhibitors with phthalazinone scaffolds were designed, synthesized and evaluated. Compound **26** was found to be the most promising for further study. Compound **26** possessed high potency (EC_{50} = 46.2 ± 3.5 nM) and low cytotoxicity.**26** possessed high MDR reversal activity towards doxorubicin-resistant K56/A02 cells. Reversal fold (RF) value reach to 44.26. **26** also increased accumulation of doxorubicin (DOX or ADM) or other MDR-related anticancer drugs with different structures. In conclusion, compound **26** deserves more research for its good features as P-gp inhibitor.

1. Introduction

Drug resistance is one of the main causes of chemotherapy failure [1]. And Multidrug resistance (MDR) accounts for a considerable proportion. Numerous studies have shown that the development of MDR is closely related to the overexpression of P-glycoprotein (P-gp, ABCB1), one of ATP-binding cassette (ABC) transport proteins [2,3]. P-glycoprotein is a cross-membrane homologous dimer composed of 1280 amino acids, each monomer consisting of a nucleotide-binding domain (NBD) and a transmembrane domain (TMD) [4,5]. P-glycoprotein acts as a drug efflux pump, leading to chemotherapy drugs going into cancer cells difficultly and decreasing the intra-cellular concentration of anticancer drugs [6,7].

P-glycoprotein inhibitors are used to help anticancer drugs evade P-gp-mediated MDR. Nowadays, three generations of P-gp inhibitors have been developed [8]. First-generation inhibitors, such as Verapamil (**1**) and Cyclosporin A (**2**), are primarily those existing drugs possessing inhibition against P-gp [9]. Such P-gp inhibition was found as side effects of drugs during research [8]. Structural modification based on first-generation inhibitors develops second-generation inhibitors that possess better selectivity and affinity but still obvious side effects [10]. For example, Dexverapamil (**3**) and Valspodar (**4**) [11] (Fig. 1). And in order to overcome inherent defects of first-generation and second-generation inhibitors, third-generation inhibitors represented by Tariquidar (**5**) and Zosuquidar (**6**) have been developed on basis of QSAR and combinatorial chemistry methods [10]. However, no P-gp inhibitors have yet been approved for marketing. Research on P-gp-mediated MDR reversal agents have been done for almost four decades, no significant progress has been made. Hence, discovery of novel P-gp inhibitors having high efficiency and safety is extremely urgent.

Studies have shown that several tyrosine kinase inhibitors (TKIs) having the structure of quinazoline can effectively inhibit P-gp activity [12,13]. Our group have designed, synthesized and evaluated novel quinazoline P-gp inhibitors. Candidate compound **LBM-11** was found possessing favorable activity, EC_{50} reaches to 57.9 ± 3.5 nM [14]. In this article, we choose the quinazoline P-gp inhibitor as lead compound, and design structure of phthalazinone as isostere to replace quinazoline in order to obtain higher activity (Fig. 2). Carbonyl oxygen in designed phthalazinone structure could provide more interaction with P-gp protein. And designed structure of amide bond is more similar to the

* Corresponding authors at: Center of Drug Discovery, State Key Laboratory of Natural Medicines, China Pharmaceutical University, 24 Tongjiaxiang, Nanjing 210009, PR China.
E-mail addresses: ydhuangwenlong@126.com (W. Huang), qianhai24@163.com (H. Qian).
[1] These authors contributed equally to this work.

https://doi.org/10.1016/j.bioorg.2019.01.039
Received 24 December 2018; Received in revised form 9 January 2019; Accepted 21 January 2019
Available online 22 January 2019

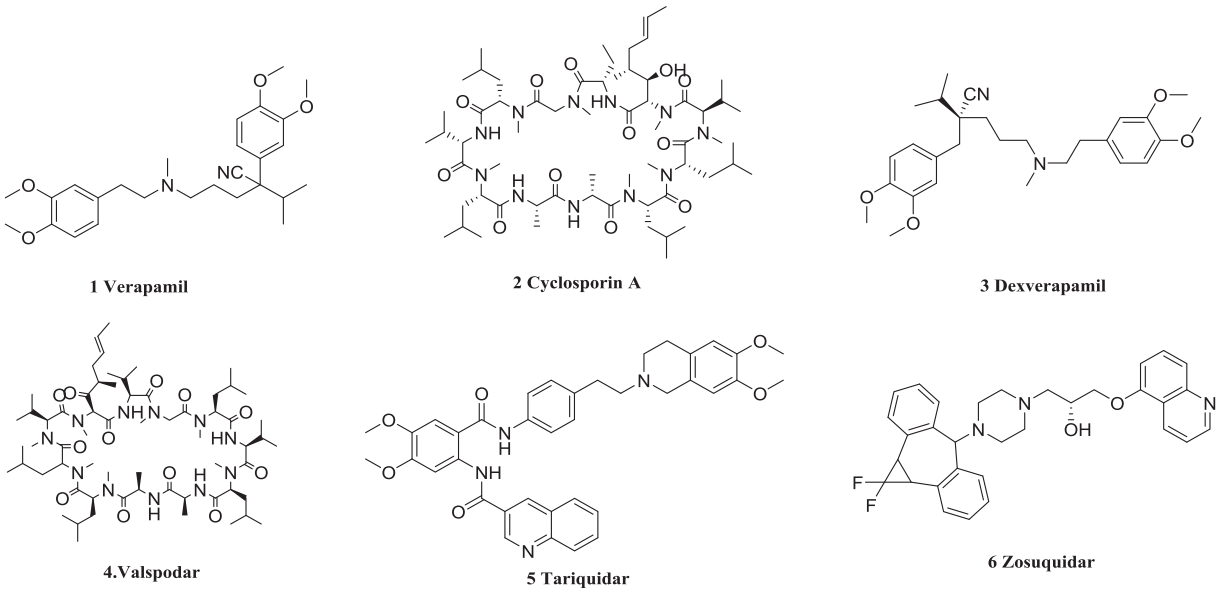

Fig. 1. Structures of P-gp inhibitors.

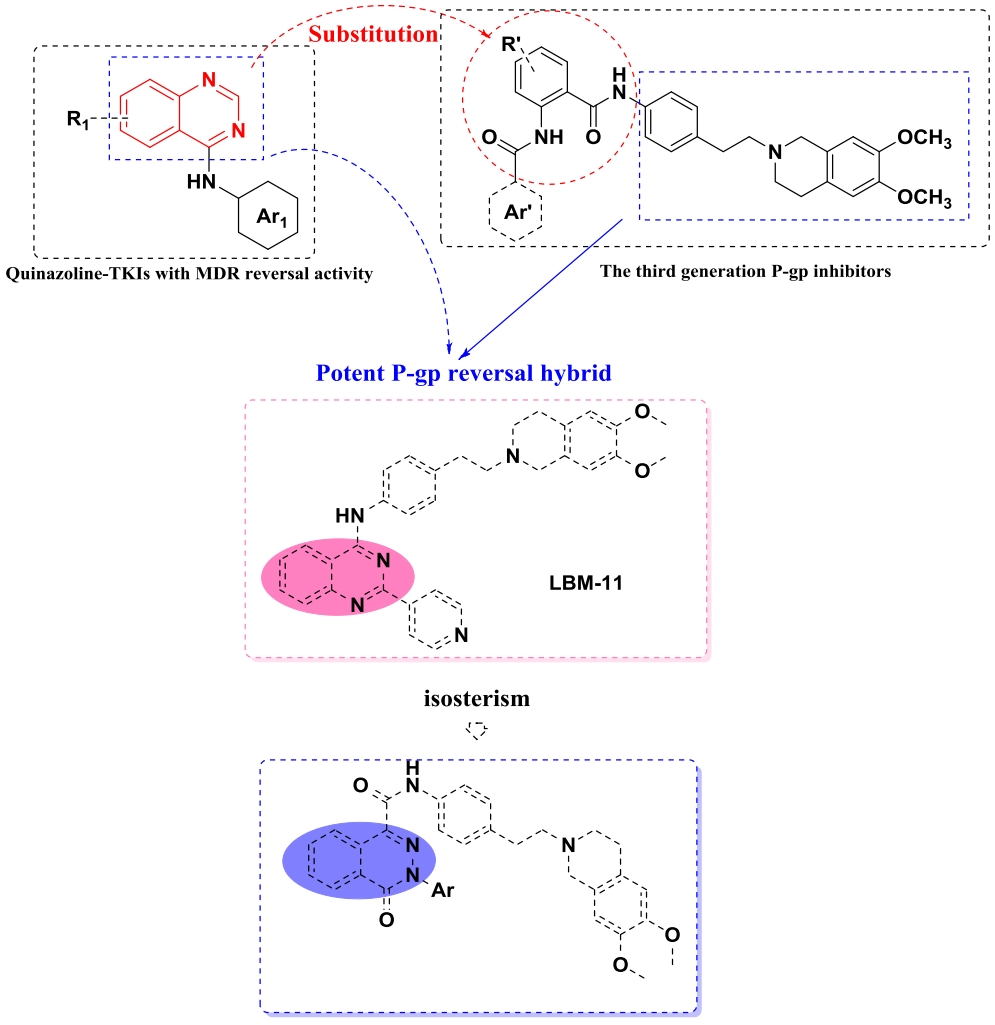

Fig. 2. Design of novel P-gp inhibitors.

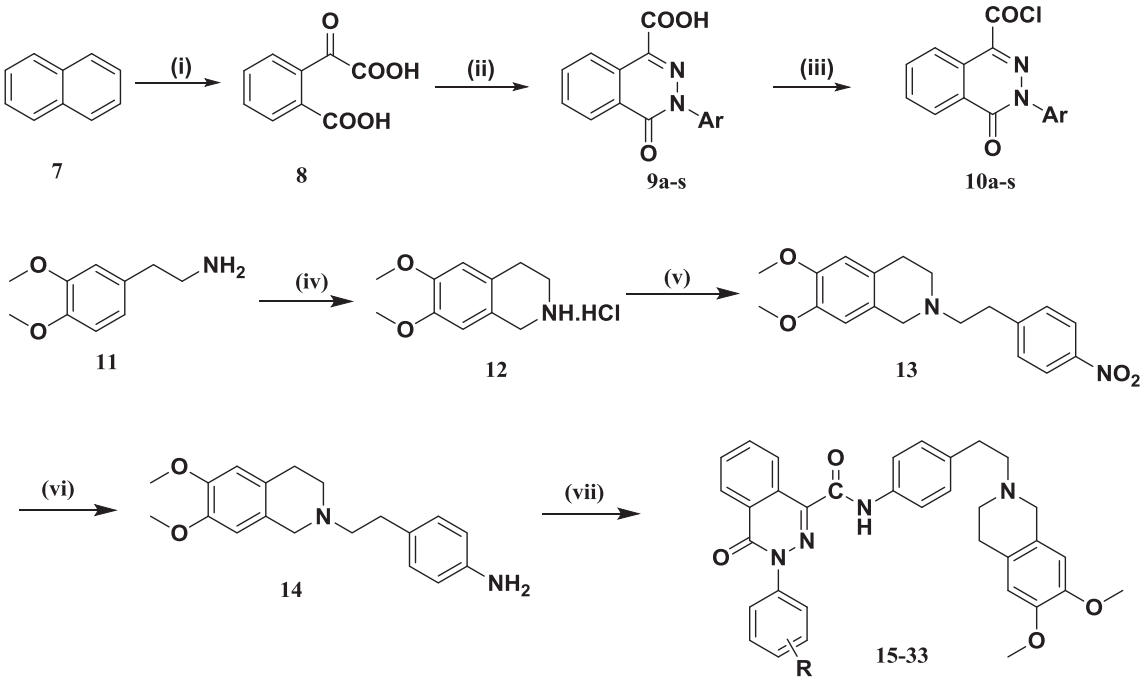

Scheme 1. Reagents and conditions: (i) 0.5 mol/L NaOH aq, $KMnO_4$, H_2O, reflux, 2 h; (ii) substituted phenyl hydrazine, EtOH, rt, 15 h; (iii) $SOCl_2$, reflux, 6 h; (iv) $(CH_2O)n$, EtOH, r.t., 3 h; con. HCl, reflux, 4 h; (v) 1-(2-bromoethyl)-4-nitrobenzene, K_2CO_3, CH_3CN, reflux, 17 h; (vi) H_2/Pd-C, DCM/EtOH, r.t., 24 h; (vii) **10a–s**, Et_3N, DCM, rt, overnight.

third-generation P-gp inhibitor, so activity is expected to reserve to the maximum extent.

2. Results and discussion

2.1. Chemistry

The synthetic route to prepare phthalazinone derivatives **15–33** is shown in Scheme 1. Intermediate **8** was prepared from Naphthalene oxidized by $KMnO_4$. The synthesized **8** was stirred in EtOH with substituted phenyl hydrazine at R.T. for 15 h to afford intermediate **9a–s** [15]. Under reflux condition, **9a–s** reacted with $SOCl_2$ to produce intermediate **10a–s**. 3,4-dimethoxyphenylethylamine and paraformaldehyde were mixed in EtOH and stirred at R.T. for 3 h and then refluxed for 4 h after acidification with concentrated hydrochloric acid to afford intermediate **12**. Under reflux conditions, intermediate **12** and 4-Nitrophenethyl bromide were reacted for 17 h to produce compound **13**. Compound **13** was reduced under hydrogen atmosphere with Pd/C as catalyst to give intermediate **14**. Add triethylamine to the mixture of **10a–s** and intermediate **14** in dichloromethane and the solution was stirred at R.T. overnight to produce target compounds **15–33**. Structures of all the target compounds are presented in Table 1.

2.2. Biological evaluation

2.2.1. Cytotoxicity assay in vitro

The effects of synthesized compounds on the viability of sensitive K562 cells and its ADM-resistant K562/A02 cells with overexpressed P-gp were determined preliminarily by the MTT assay. As present in Table 2, Most of the tested compounds show no cytotoxicity to two strains of cells. IC_{50} value is greater than 50 μM. Compound **28** and **29** show weak cytotoxicity to K562 cells. Positive control Verapamil (VRP) shows certain cytotoxicity to both K562 and K562/A02 cells.

2.2.2. MDR reversal activity test on K562/A02 cells in vitro

According to the results of cytotoxicity test, all target compounds show no cytotoxicity at the concentration of 2 μM. So target compounds are tested MDR reversal activity towards ADM-resistant K562/A02 cells with overexpressed P-gp at such concentration. Results are presented in Table 3. All target compounds show MDR reversal activity at 2 μM. Most of the compounds are superior to the control Verapamil. Among them, compound **15**, **20**, **23**, **25**, **26** and **28** are far better than Verapamil. These six compounds are tested MDR reversal activity at concentration of 100 nM. As shown in Table 4, they still possess potent MDR reversal activity even at a low concentration. Especially for compound **26**, Reversal fold (RF) value reach 20.

IC_{50} ($\bar{x}$ ± s, n = 3) is determined by MTT assay testing cytotoxicity on K562/A02 cells when 2 μM tested compound is combined on the cells with doxorubicin of different concentrations; Reversal fold (RF) = IC_{50} of doxorubicin with no reversal agents existing / IC_{50} of doxorubicin with reversal agents existing; 0.1% DMSO is blank control.

IC_{50} ($\bar{x}$ ± s, n = 3) is determined by MTT assay testing cytotoxicity on K562/A02 cells when 2 μM tested compound is combined on the cells with doxorubicin of different concentrations; Reversal fold (RF) = IC_{50} of doxorubicin with no reversal agents existing / IC_{50} of doxorubicin with reversal agents existing; 0.1% DMSO is blank control.

2.2.3. Dose-effect relationship research of MDR reversal activity of compound 26

As can be seen from the test results presented in the Fig. 3, compound **26** still show weak reversal activity at the concentration of 7.8 nM. EC_{50} refers to the concentration of inhibitor required to reduce the IC_{50} of doxorubicin by half compared with a control without a inhibitor [16]. According to reversal activity data at different concentration, EC_{50} was calculated as 46.2 ± 4.7 nM.

2.2.4. Selective index of compound 26

As shown in the Fig. 4, compound **26** shows no cytotoxicity to GES-1 cells (normal cell). Even at the concentration of 100 μM, survival rate of GES-1 is still higher than 80%. After calculation, selective index is greater than 2165, indicating that compound **26** is also safe for normal cells when it plays the role of MDR reversing.

Table 1
Structures of target compounds.

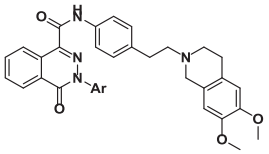

Compound	Ar	Compound	Ar	Compound	Ar
15		**22**		**29**	
16		**23**	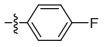	**30**	
17		**24**		**31**	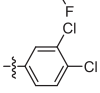
18		**25**		**32**	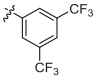
19		**26**	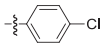	**33**	
20	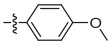	**27**	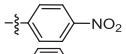		
21		**28**	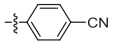		

Table 2
Cytotoxicity of target compounds towards K562 and K562/A02 cells.

Compound	IC_{50} (μM)		Compound	IC_{50} (μM)	
	K562	K562/A02		K562	K562/A02
15	> 100	> 100	**26**	> 100	> 100
16	> 100	> 100	**27**	72.19 ± 3.39	83.42 ± 2.40
17	> 100	> 100	**28**	43.75 ± 1.35	> 100
18	> 100	> 100	**29**	38.23 ± 2.10	73.01 ± 3.29
19	> 100	> 100	**30**	64.15 ± 1.77	84.81 ± 2.94
20	> 100	> 100	**31**	> 100	> 100
21	> 100	> 100	**32**	> 100	> 100
22	> 100	> 100	**33**	69.86 ± 4.03	> 100
23	78.35 ± 4.42	> 100	VRP	34.96 ± 2.24	31.71 ± 2.37
24	62.64 ± 2.63	> 100	LBM-11	4.23 ± 0.36	12.30 ± 0.73
25	57.22 ± 3.04	> 100	ADM	0.63 ± 0.09	67.28 ± 2.69

Table 3
MDR reversal activity of target compounds on K56/A02 cells at concentration of 2 μM.

Compound (2.0 μM)	IC_{50}/ADM (μM)	RF	Compound (2.0 μM)	IC_{50}/ADM (μM)	RF
15	2.22 ± 0.37	30.31	**26**	1.52 ± 0.26	44.26
16	3.38 ± 0.14	19.90	**27**	2.43 ± 0.37	27.69
17	3.06 ± 0.25	21.99	**28**	2.07 ± 0.12	32.50
18	5.39 ± 0.96	12.48	**29**	6.16 ± 0.31	10.92
19	2.83 ± 0.32	23.77	**30**	11.81 ± 0.28	5.70
20	1.89 ± 0.21	35.60	**31**	13.54 ± 0.56	4.97
21	3.93 ± 0.64	17.12	**32**	21.46 ± 2.09	3.14
22	4.82 ± 0.59	13.96	**33**	4.23 ± 0.75	15.91
23	2.10 ± 0.32	32.04	VRP (5.0 μM)	14.88 ± 1.50	4.52
24	12.46 ± 2.78	5.40	LBM-11	2.27 ± 0.43	29.64
25	2.48 ± 0.13	27.13	0.1% DMSO	67.28 ± 4.19	1.00

2.2.5. MDR reversal activity test on other P-gp-mediated anticancer-drug-resistant cells

As shown in the Fig. 5, compound **26** can obviously enhance cytotoxicity of Paclitaxel (PTX), Vinblastine (VLB), Daunorubicin (DNR) to drug-resistant cells. PTX, VLB and DNR are easily pumped by P-gp out of cancer cells. When compound **26** was combined with these anticancer drugs, it can increase their concentration in cancer cells so cytotoxicity was significantly increased. However, Cyclophosphamide (CTX) is not substrate of P-gp, combined compound **26** cannot influence its concentration in cells. These results indicate that inhibition of P-gp function by compound **26** is the cause of drug resistance reversal.

*2.2.6. Effect of compound **26** on doxorubicin accumulation*

Effect of compound **26** on doxorubicin accumulation in drug-resistant cells can been seen in Fig. 6. Doxorubicin accumulation is significantly more in doxorubicin-sensitive K562 cells than in doxorubicin-resistant K562/A02 cells, it is about 5.9 folds. Compared with blank

Table 4
MDR reversal activity of preferred compounds on K56/A02 cells at concentration of 100 nM.

Compound (100 nM)	IC_{50}/ADM (μM)	RF	Compound (100 nM)	IC_{50}/ADM (μM)	RF
15	8.34 ± 0.91	7.75	**28**	5.36 ± 0.37	12.05
20	4.39 ± 0.42	14.72	VRP (5.0 μM)	15.37 ± 0.84	4.20
23	7.15 ± 0.24	9.04	LBM-11	4.20 ± 0.25	15.39
25	9.93 ± 1.30	6.51	0.1% DMSO	64.61 ± 3.41	1.00
26	3.26 ± 0.13	19.82			

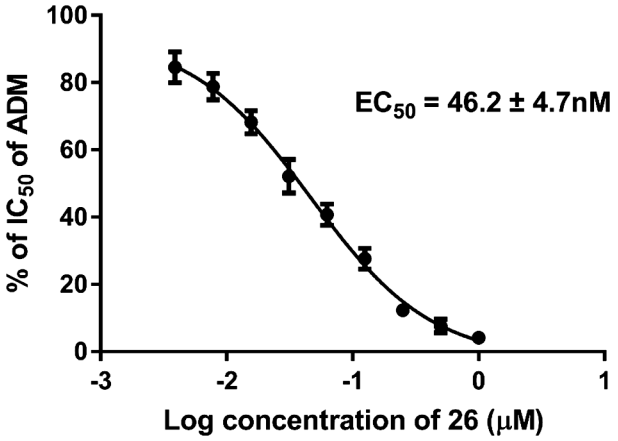

Fig. 3. EC_{50} value of **26** in reversing ADM-resistance in K562/A02 cells. The percent of IC_{50} of ADM = [(IC_{50} of ADM at each modulator concentration/IC_{50} of ADM without modulator) × 100%)]. EC_{50} refers to the concentration of modulator that can reduce the % of IC_{50} of ADM by half. Each data point is presented as mean ± SD of three independent tests.

control, in different experiment group with different concentration of reversal agents added, doxorubicin accumulation in K562/A02 cells increased to different degrees. Compound **26** can significantly increase doxorubicin accumulation in doxorubicin-resistant K562/A02 cells even at the low concentration of 0.1 μM, while Verapamil increases doxorubicin accumulation only at the high concentration of 2.0 μM. These results indicates that compound **26** inhibits the transport function of P-gp, causing significant doxorubicin accumulation in drug-resistant cells.

2.2.7. Structure-activity relationship research of the target compounds 15–33

Based on reversal activity results, structure-activity relationship is analyzed as below (Fig. 7): Structure of component A is common in third-generation P-gp inhibitors, which plays a crucial role as important pharmacophore; When phthalazinone substitutes quinazoline in component B, reversal activity of compounds is enhanced on the whole; When component C is phenyl ring, number and position of substituents on the ring have a significant influence on the reversal activity. When substituted at 3-positon of the phenyl ring, reversal activity is kept or slightly reduced. Activity is significantly enhanced when substituted at 4-position, and becomes strongest with 4-Cl substituted. Multiple substituents reduce activity and such reduction is obvious when substituents are electron withdrawing group.

2.2.8. Docking experiments for compound 26

Docking experiments have been conducted to study interaction between P-gp protein and Compound **26** (Fig. 8). Results show that Compound 26 occupied hydrophobic pocket of P-gp protein. Compound **26** has H-bond interaction with residue GLN 721, and Pi-Pi stacking interaction with TYR 303. More importantly, tertiary amine N atom of

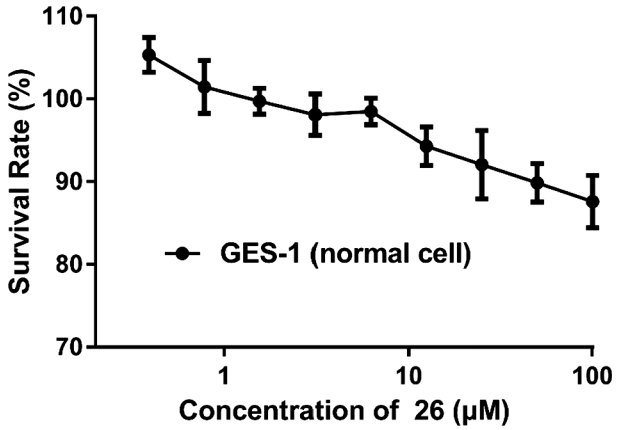

Fig. 4. The survival rate of different concentrations of **26** was determined in GES-1 cells. Data were analyzed with GraphPad Prism 5.0 software and presented as mean ± SD for three independent tests.

Compound **26** could capture hydrogen ion, forming positive charge center, to interact with residue PHE 728, which is essential to maintain activity.

3. Conclusion

In this study, a series of novel P-gp-mediated MDR modulators with phthalazinone scaffolds were designed and synthesized. All the structures of the synthesized compound were characterized by NMR, HRMS. Biological evaluation in vitro demonstrated that a few compounds possess potent MDR reversal activity. In particular, compound **26** exhibited high activity against doxorubicin-resistant K562/A02 cells with a low EC_{50} (46.2 ± 4.7 nM). Compound **26** show no cytotoxicity towards normal cells (IC_{50} > 100 μM). Calculated SI of compound**26** was very high (> 2165). Compound **26** also exhibited reversal activity on other anticancer drugs that may have different structures and mechanisms of action such as P-gp substrates (PTX, VLB, DNR) but exhibited no activity on the non-P-gp substrate CTX. Compound **26** increased doxorubicin accumulation in drug-resistant cells, which demonstrates that it can inhibit the transfer function of P-gp.

4. Experimental section

4.1. Material and methods

4.1.1. Materials

3-(4,5-Dimethylthiazol-2-yl)-2,5-diphenyltetrazolium bromide (MTT), doxorubicin (DOX), daunorubicin (DNR), vinblastine (VLB), paclitaxel (PTX), cyclophosphamide (CTX), verapamil (VRP) and dimethyl sulfoxide (DMSO) were purchased from Sigma-Aldrich (St. Louis, MO, USA). RPMI-1640s and FBS were from GIBCO, USA. Human leukemia sensitive cell line K562 and its doxorubicin-selected P-gp overexpressing daughter cell line K562/A02 were kindly provided by Professor Bao-An Chen (Department of Hematology, The Affiliated Zhong-Da Hospital, Southeast University (Nanjing, China). The cell lines were grown in RPMI-1640 medium supplemented with 10% heat-inactivated fetal bovine serum (FBS) in a humidified incubator at 37 °C with 5% CO_2. To confirm drug resistance characteristics, 1 mg/mL ADM was added to K562/A02 cultures and maintained in drug-free medium for 2 weeks before usage. The cells in exponential growth can be used for experiments.

4.1.2. Methods

4.1.2.1. Cytotoxicity assay. Cell viability was determined by MTT method with a minor modification [17–20]. K562 and K562/A02 cells during logarithmic growth phase were seeded in 96-well

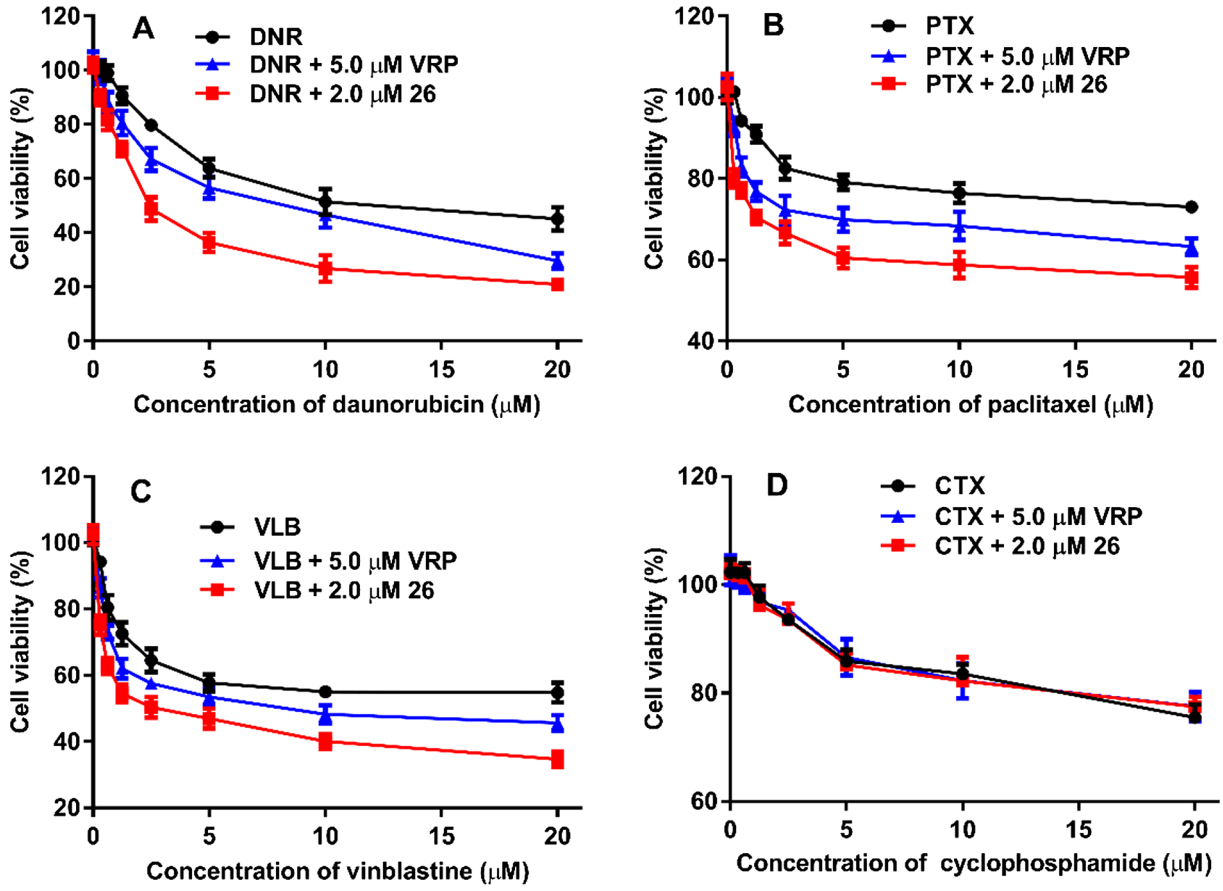

Fig. 5. MDR reversal activity of **26** on P-gp-mediated resistance to other anticancer agents. DNR, PTX, and VLB are P-gp substrates, whereas CTX is not. Each data point is presented as mean ± SD of three independent tests.

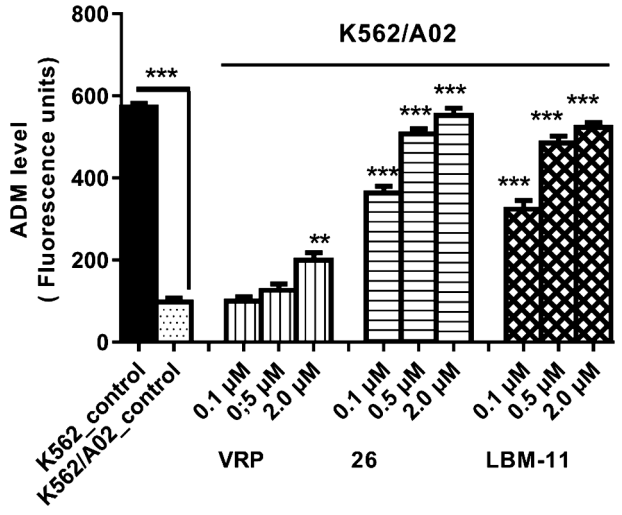

Fig. 6. Effect of compound **26** on intracellular doxorubicin accumulation in K562/A02 cells. 0.1% DMSO was used as negative control. VRP was chosen as positive controls. N = 3 independent experiments. The results are presented as the mean ± standard error of mean: (**) P < 0.01, (***) P < 0.001 relative to the negative control (K562/A02).

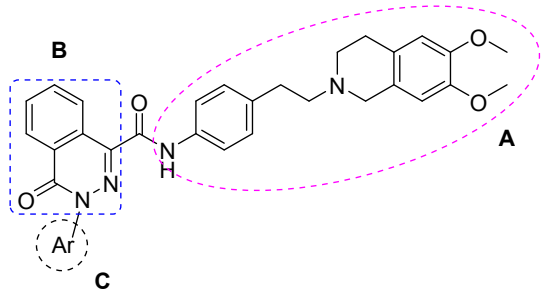

Fig. 7. Structure-activity relationship of target compounds:(A) Crucial pharmacophore of third-generation P-gp inhibitors; (B) Phthalazinone enhances reversal activity; (C) Different substituents influence activity significantly.

microtiter plates at 3×10^4 cells per well. P-gp inhibitors were prepared as 5 mM DMSO stocks. In the MTT assay for MDR reversal experiments, cells were incubated in the presence of P-gp inhibitors for 48 h. MTT dye (10 μL of 2.5 mg/mL in PBS) was added to each well 4 h prior to experiment termination in a 37 °C incubator containing 5% CO_2. The plates were then centrifuged at 1500 rpm for 15 min and the supernatant was discarded without disturbing the formazan crystals and cells in the wells, while the MTT formazan crystals were dissolved in 150 μL of DMSO and the plates agitated on a plate shaker for 5 min. The optical density (OD) was read on a microplate reader (Thermo, USA) with a wavelength of 490 nm. Cell inhibition rate was calculated. The IC_{50} values of the compounds for cytotoxicity were calculated by GraphPad Prism 5.0 software (GraphPad software, San Diego, CA, USA) from the dose-response curves. Cell inhibition rate = 1 − (average OD of experimental group/average OD of control group) * 100%.

4.1.2.2. MDR reversal activity test. Method is similar to cytotoxicity assay. K562 and K562/A02 cells during logarithmic growth phase were seeded in 96-well microtiter plates at 3×10^4 cells per well. P-gp inhibitors were prepared as 5 mM DMSO stocks. In the MTT assay for MDR reversal experiments, cells were incubated in the presence of

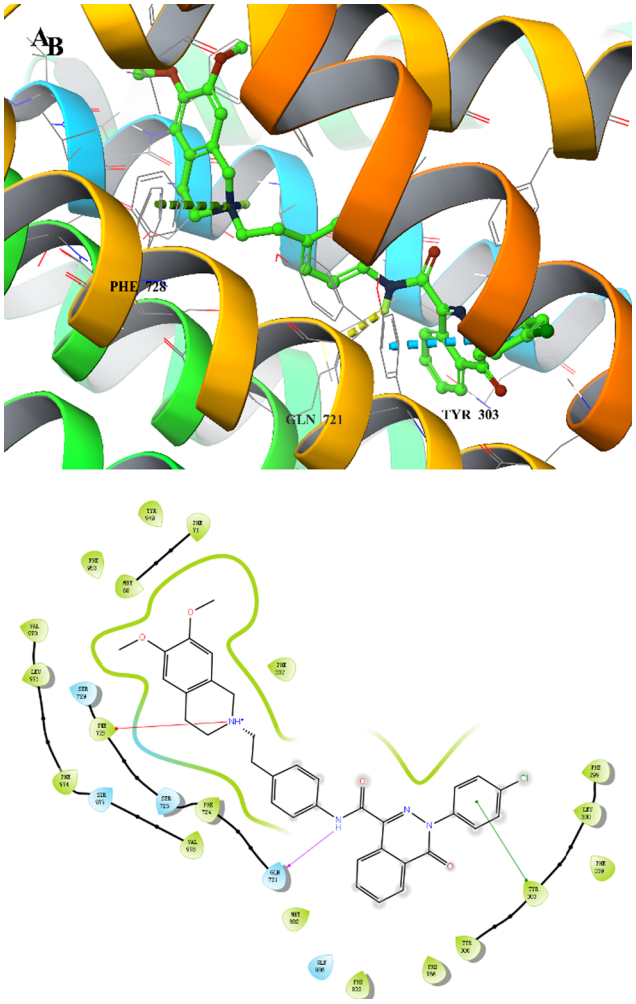

Fig. 8. Structure docking results with P-gp for **Compound 26**. (A) 3D diagram (B) 2D diagram.

anticancer agents (DOX, DNR, VLB, PTX, or CTX) with P-gp inhibitors for 48 h. MTT dye (10 μL of 2.5 mg/mL in PBS) was added to each well 4 h prior to experiment termination in a 37 °C incubator containing 5% CO_2. The plates were then centrifuged at 1500 rpm for 15 min and the supernatant was discarded without disturbing the formazan crystals and cells in the wells, while the MTT formazan crystals were dissolved in 150 μL of DMSO and the plates agitated on a plate shaker for 5 min. The optical density (OD) was read on a microplate reader (Thermo, USA) with a wavelength of 490 nm. Cell inhibition rate was calculated. The IC_{50} values of the compounds for cytotoxicity were calculated by GraphPad Prism 5.0 software (GraphPad software, San Diego, CA, USA) from the dose-response curves. Cell inhibition rate = 1 − (average OD of experimental group/average OD of control group) * 100%. Reversal fold (RF) = IC_{50}A/IC_{50}B. IC_{50}A refers to IC_{50} of doxorubicin towards K562/A02 cells with no reversal agents existing. IC_{50}B refers to IC_{50} of doxorubicin towards K562/A02 cells with reversal agents existing.

4.1.2.3. Dose-effect relationship research of MDR reversal activity. The test compound was diluted with serum-containing medium to a final concentration of 5.0 μM, 2.5 μM, 1.25 μM, 0.625 μM, 0.31 μM, 0.156 μM, 0.078 μM, 0.04 μM, 0.02 μM and 0.01 μM. MDR reversal activity of the compound is tested at different concentration of test compound. Detailed method is same as Section 4.1.2.2.

4.1.2.4. Selective index research. IC_{50} value of preferred compound towards GES-1 cells is determined by MTT method. Detailed method is same as Section 4.1.2.1. Selective index (IS) = IC_{50}A/EC_{50}B. IC_{50}A refers to IC_{50} of preferred compound towards GES-1 cells. EC_{50}B refers to the concentration of preferred compound that can reduce the % of IC_{50} of ADM by half.

4.1.2.5. Doxorubicin accumulation assay in vitro. Reported procedure was employed with minor modification to detect concentration of doxorubicin in cells [16,21]. 2×10^5 cells of K562 and K562/A02 were incubated with 20.0 μM DOX and different concentrations of tested compound and VRP for 150 min at 37 °C, with 0.1% DMSO as a negative control. After incubation, the cells were washed with cold PBS and lysed with lysis buffer (0.75 M HCl, 0.2% Triton-X100 in 2-propanol). The fluorescence level of DOX in the lysate was measured by fluorescence spectrophotometer (RF-5301 PC, Shimadzu) using an excitation and an emission wavelength pair of 460 and 587 nm.

4.1.2.6. Docking experiments. Receptor protein (PDB ID:3G60) was prepared and optimized using relevant module by Schrodinger software. Receptor Grid Generation Module was used to generate docking area. Structure of ligands were drawn by ChemOffice2014 software and prepared using LigPrep module. In the end, molecular docking between ligands and receptor was conducted with extra precision.

4.2. Apparatus and chemistry

Melting points were taken on a RY-1 melting-point apparatus and were uncorrected; NMR s1pectra were recorded on a Bruker ACF300/500 MHz instrument, tetramethylsilane (TMS) as internal standard; Purification by column chromatography were carried out over silica gel (100–200 or 200–300 mesh); Reactions were monitored by thin layer chromatography on GF/UV254 plates and were visualized using UV light at 254 or 365 nm; ESI-MS data was recorded on Waters ACQUITY UPLC systems with mass (Waters, Milford, MA). All chemical reagents were obtained from commercial sources and used without purification unless otherwise indicated.

4.3. Synthesis

4.3.1. Synthesis of 2-(carboxycarbonyl)benzoic acid (8)

Naphthalene (16.0 g, 125.0 mmol) was dissolved in 0.5 N NaOH (250 mL) and refluxed. Potassium permanganate (106 g, 670.0 mmol) was dissolved in 750 mL of boiling water and added dropwise to the refluxing solution in 1.5 h. after completion of the dropwise addition, the reaction was continued for 30 min to complete oxidation, and the reaction was quenched by adding 100 mL of ethanol, and the mixture was cooled to room temperature and suction filtered. The filter cake was acidified with 30% hydrochloric acid, and extracted with ethyl acetate (75 mL × 3). The organic layers were combined, dried with anhydrous sodium sulfate. Solvent was evaporated under reduced pressure to give compound **8**. Yield 35.0%, white solid, m.p. 142–144 °C

*4.3.2. Preparation of intermediates **9a–s** and **10a–s***

Prepare a mixed solution of 30 mL of ethanol and water (1:2), dissolve the corresponding aromatic hydrazine hydrate (10.30 mmol) in 20 mL of the mixed solution and drop into the 10 mL mixed solution of compound **8**. The mixture was stirred at room temperature for 15 h. Precipitation was filtered and washed with dichloromethane twice, then vacuum dried to give intermediates **9a–s**. To the corresponding intermediate **9a–s** (10.0 mmol), thionyl chloride (15 mL) was added and the mixture was heated to reflux for 5–7 h. Extra liquid was evaporated under reduced pressure to give compound **10a–s**

4.3.3. Synthesis of 4-[2-(6,7-Dimethoxy-3,4-dihydro-1H-isoquinolin-2-yl)-ethyl]phenylamine (14)

4.3.3.1. Synthesis of 6,7-Dimethoxy-1,2,3,4-tetrahydro-isoquinoline hydrochloride (12). To a 250 mL single-necked flask was added 3,4-dimethoxyphenethylamine (**11**) (18.1 g, 100 mmol), paraformaldehyde (3.6 g, 120 mmol), and anhydrous ethanol (30 mL). After stirring at room temperature for 3 h, the mixture was adjusted to pH = 2 with concentrated hydrochloric acid, and then refluxed for 4 h. Cooling and filtering to give white crystalline hydrochloride solid 14.2 g. Yield 61.8%.

4.3.3.2. Synthesis of 6,7-dimethoxy-2-(4-nitrophenethyl)-1,2,3,4-tetrahydroisoquinoline (13). Mixture of 4-nitrophenethyl bromide (2.42 g, 10 mmol), compound **12** (2.41 g, 10.5 mmol) and anhydrous potassium carbonate (3.48 g, 25.2 mmol) were heated and refluxed in acetonitrile (50 mL) for 18 h. The mixture was cooled, filtered, and the filter cake was washed with dichloromethane. The filtrate was evaporated under reduced pressure to obtain the yellow solid residue, recrystallized by ethanol to obtain the yellow acicular solid 2.76 g. Yield 81.2%.

*4.3.3.3. Preparation of **14***. Compound **13** (11.02 g, 32.2 mmol) was dissolved in ethanol/dichloromethane (1:1, 60 mL) mixture, and hydrogen reduction reaction was catalyzed by Pd/C (0.58 g) at room temperature for 48 h. Dichloromethane washed the filter cake. The filtrate was evaporated under reduced pressure to obtain a light yellow solid. Recrystallization by dichloromethane/petroleum ether resulted in a pale white solid of 7.9 g. Yield 79.0%.

4.3.4. Preparation of target compounds 15–33

Compound **14** (0.31 g, 1 mmol), triethylamine (1.2 mmol) was dissolved in dichloromethane (10 mL). Under the condition of ice bath, it was added by drops into dichloromethane solution of corresponding compound **10a–s** (1.1 mmol). After addition was completed, mixture was moved to room temperature and continued to react for 10 h. Reaction solution was washed with 10% potassium carbonate (20 mL × 3), saturated saline (20 mL × 3), The organic layer was dried with anhydrous sodium sulfate, then the solvent was removed by vacuum evaporation to obtain the crude product. Then the column chromatography CH_2Cl_2/MeOH (80:1) was used to obtain compound **15–33**.

4.3.4.1. N-(4-(2-(6,7-dimethoxy-3,4-dihydroisoquinolin-2(1H)-yl)ethyl) phenyl)-4-oxo-3-phenyl-3,4-dihydrophthalazine-1-carboxamide (15). Yield 65.9%, light yellow solid, m.p. 170–172 °C. ^{1}H NMR (300 MHz, DMSO-d_6) δ: 10.61 (s, 1H), 8.52–8.25 (m, 2H), 8.13–7.89 (m, 2H), 7.77 (d, J = 7.4 Hz, 2H), 7.68 (d, J = 8.1 Hz, 2H), 7.55 (t, J = 7.4 Hz, 2H), 7.47 (d, J = 7.0 Hz, 1H), 7.27 (d, J = 8.0 Hz, 2H), 6.64 (d, J = 6.5 Hz, 2H), 3.70 (s, 6H), 3.54 (s, 2H), 2.82 (s, 2H), 2.69 (s, 6H) ; ^{13}C NMR (75 MHz, DMSO-d_6) δ: 161.45, 141.26, 140.42, 136.56, 136.10, 134.16, 132.61, 128.94, 128.57, 127.87, 126.84, 126.31, 126.08, 125.88, 120.23, 111.76, 109.96, 59.46, 55.43, 55.05, 50.53, 32.42, 28.28; ESI-MS m/z: 561.6 $[M+H]^+$. Anal. Calcd for $C_{34}H_{32}N_4O_4$: C, 72.84; H, 5.75; N, 9.99. Found: C, 72.82; H, 5.77; N, 9.98.

4.3.4.2. N-(4-(2-(6,7-dimethoxy-3,4-dihydroisoquinolin-2(1H)-yl)ethyl) phenyl)-4-oxo-3-(m-tolyl)-3,4-dihydrophthalazine-1-carboxamide (16). Yield 70.3%, yellow solid, m.p. 112–114 °C. ^{1}H NMR (300 MHz, DMSO-d_6) δ: 10.64 (s, 1H), 8.51–8.28 (m, 2H), 8.07–7.89 (m, 2H), 7.68 (d, J = 7.6 Hz, 2H), 7.55 (d, J = 9.0 Hz, 2H), 7.43 (s, 2H), 7.27 (d, J = 7.5 Hz, 2H), 6.64 (d, J = 5.8 Hz, 2H), 3.70 (s, 6H), 3.54 (s, 2H), 2.78 (d, J = 19.8 Hz, 2H), 2.69 (s, 6H), 2.40 (s, 3H); ^{13}C NMR (75 MHz, DMSO-d_6) δ: 161.48, 158.06, 147.10, 146.71, 141.21, 140.39, 138.10, 136.55, 136.13, 134.11, 132.57, 128.93, 128.51, 128.39, 127.91, 126.79, 126.42, 125.89, 123.26, 120.23, 111.75, 109.96, 59.47, 55.43, 55.04, 50.52, 32.43, 28.28, 20.86; ESI-MS m/z: 575.6 $[M+H]^+$. Anal. Calcd for $C_{35}H_{34}N_4O_4$: C, 73.15; H, 5.96; N, 9.75. Found: C, 73.16; H, 5.98; N, 9.73.

4.3.4.3. N-(4-(2-(6,7-dimethoxy-3,4-dihydroisoquinolin-2(1H)-yl)ethyl) phenyl)-4-oxo-3-(p-tolyl)-3,4-dihydrophthalazine-1-carboxamide (17). Yield 54.8%, yellow solid, m.p. 145–147 °C.^{1}H NMR (300 MHz, DMSO-d_6) δ: δ 10.60 (s, 1H), 8.41 (t, J = 6.9 Hz, 2H), 8.08–7.92 (m, 2H), 7.66 (dd, J = 8.3, 7.6 Hz, 4H), 7.36–7.26 (m, 4H), 6.64 (d, J = 4.0 Hz, 2H), 3.70 (s, 6H), 3.55 (s, 2H), 2.80 (s, 2H), 2.70 (s, 6H), 2.40 (s, 3H); ^{13}C NMR (75 MHz, DMSO-d_6) δ:161.49, 158.13, 147.05, 146.81, 141.18, 140.37, 138.11, 136.56, 136.09, 134.10, 132.57, 128.93, 128.53, 128.39, 127.88, 126.85, 126.76, 126.55, 125.87, 123.25, 120.22, 111.68, 109.90, 59.46, 55.40, 55.02, 50.50, 32.39, 28.25, 20.85; ESI-MS m/z: 575.6 $[M+H]^+$. Anal. Calcd for $C_{35}H_{34}N_4O_4$: C, 73.15; H, 5.96; N, 9.75. Found: C, 73.17; H, 5.97; N, 9.77.

4.3.4.4. N-(4-(2-(6,7-dimethoxy-3,4-dihydroisoquinolin-2(1H)-yl)ethyl) phenyl)-3-(2-ethylphenyl)-4-oxo-3,4-dihydrophthalazine-1-carboxamide (18). Yield 56.8%, yellow solid, m.p. 119–121 °C.^{1}H NMR (300 MHz, DMSO-d_6) δ: 10.50 (s, 1H), 8.39 (s, 2H), 8.04 (d, J = 7.3 Hz, 2H), 7.64 (d, J = 8.0 Hz, 2H), 7.46 (s, 4H), 7.27 (s, 2H), 6.64 (d, J = 6.5 Hz, 2H), 3.70 (s, 6H), 3.54 (s, 2H), 2.75 (d, J = 32.8 Hz, 8H), 1.23 (s, 3H), 1.11 (d, J = 7.3 Hz, 2H); ^{13}C NMR (75 MHz, DMSO-d_6) δ: 161.11, 158.90, 157.67, 150.55, 147.11, 146.87, 137.21, 135.66, 132.98, 130.87, 129.50, 128.58, 127.85, 126.66, 125.92, 125.31, 122.93, 122.00, 113.69, 111.74, 109.97, 59.53, 55.45, 55.09, 50.52, 32.24, 28.16, 13.67; ESI-MS m/z: 589.7 $[M+H]^+$. Anal. Calcd for $C_{36}H_{36}N_4O_4$: C, 73.45; H, 6.16; N, 9.52 Found: C, 73.44; H, 6.15; N, 9.53.

4.3.4.5. N-(4-(2-(6,7-dimethoxy-3,4-dihydroisoquinolin-2(1H)-yl)ethyl) phenyl)-3-(3-methoxyphenyl)-4-oxo-3,4-dihydrophthalazine-1-carboxamide (19). Yield 54.8%, yellow solid, m.p. 117–119 °C.^{1}H NMR (300 MHz, DMSO-d_6) δ: 10.65 (s, 1H), 8.40 (s, 2H), 8.02 (d, J = 9.2 Hz, 2H), 7.68 (d, J = 7.9 Hz, 2H), 7.44 (d, J = 8.0 Hz, 1H), 7.41–7.17 (m, 4H), 7.04 (d, J = 7.7 Hz, 1H), 6.64 (d, J = 6.1 Hz, 2H), 3.82 (s, 3H), 3.69 (s, 6H), 3.54 (s, 2H), 2.82 (s, 2H), 2.69 (s, 6H); ^{13}C NMR (75 MHz, DMSO-d_6) δ: 161.45, 159.34, 158.29, 158.12, 146.99, 144.66, 146.13, 142.30, 140.10, 136.54, 136.10, 134.04, 132.57, 129.29, 128.94, 127.95, 126.84, 126.63, 126.29, 125.89, 120.21, 118.39, 114.44, 113.52, 112.17, 111.75, 109.96, 59.51, 55.44, 55.07, 50.53, 32.43, 28.29, 20.64; ESI-MS m/z: 591.6 $[M+H]^+$. Anal. Calcd for $C_{35}H_{34}N_4O_5$: C, 71.17; H, 5.80; N, 9.49. Found: C, 71.16; H, 5.83; N, 9.52.

4.3.4.6. N-(4-(2-(6,7-dimethoxy-3,4-dihydroisoquinolin-2(1H)-yl)ethyl) phenyl)-3-(4-methoxyphenyl)-4-oxo-3,4-dihydrophthalazine-1-carboxamide (20). Yield 61.7%, light brown solid, m.p. 128–130 °C.^{1}H NMR (300 MHz, DMSO-d_6) δ: 10.59 (s, 1H), 8.40 (t, J = 7.7 Hz, 2H), 8.07–7.90 (m, 2H), 7.68 (d, J = 8.8 Hz, 4H), 7.27 (d, J = 8.2 Hz, 2H), 7.08 (d, J = 8.9 Hz, 2H), 6.64 (d, J = 6.6 Hz, 2H), 3.83 (s, 3H), 3.70 (s, 6H), 3.54 (s, 2H), 2.80 (d, J = 7.4 Hz, 2H), 2.69 (s, 6H); ^{13}C NMR (75 MHz, DMSO-d_6) δ: 161.53, 158.59, 158.18, 147.16, 146.90, 140.11, 136.41, 136.15, 134.27, 133.99, 132.47, 128.92, 127.89, 127.34, 126.89, 126.76, 126.41, 126.22, 125.83, 120.22, 113.68, 111.78, 109.99, 59.30, 55.42, 54.90, 50.43, 32.29, 28.12; ESI-MS m/z: 591.3 $[M+H]^+$. Anal. Calcd for $C_{35}H_{34}N_4O_5$: C, 71.17; H, 5.80; N, 9.49. Found: C, 71.17; H, 5.81; N, 9.51.

4.3.4.7. N-(4-(2-(6,7-dimethoxy-3,4-dihydroisoquinolin-2(1H)-yl)ethyl) phenyl)-3-(2-fluorophenyl)-4-oxo-3,4-dihydrophthalazine-1-carboxamide

(21). Yield 69.2%, light yellow solid, m.p. 187–189 °C.^{1}H NMR (300 MHz, DMSO-d_6) δ: 10.65 (s, 1H), 8.49–8.31 (m, 2H), 8.12–7.96 (m, 2H), 7.77 (s, 1H), 7.67 (d, J = 7.1 Hz, 2H), 7.58 (s, 1H), 7.52–7.36 (m, 2H), 7.27 (d, J = 7.5 Hz, 2H), 6.65 (d, J = 6.0 Hz, 2H), 3.70 (s, 6H), 3.54 (s, 2H), 2.81 (s, 2H), 2.69 (s, 6H); ^{13}C NMR (75 MHz, DMSO-d_6) δ: 161.04, 159.68, 146.77, 146.36, 140.81, 136.47, 136.03, 134.47, 130.70, 129.55, 128.93, 127.34, 126.82, 126.63, 125.89, 125.02, 120.24, 116.20, 115.87, 111.76, 109.97, 109.79, 108.13, 59.45, 58.65, 55.44, 55.05, 50.52, 32.42, 28.06; ESI-MS *m/z*: 579.6 [M + H]$^+$. Anal. Calcd for $C_{34}H_{31}FN_4O_4$: C, 70.57; H, 5.40; N, 9.68. Found: C, 70.56; H, 5.42; N, 9.69.

4.3.4.8. N-(4-(2-(6,7-dimethoxy-3,4-dihydroisoquinolin-2(1H)-yl)ethyl) phenyl)-3-(3-fluorophenyl)-4-oxo-3,4-dihydrophthalazine-1-carboxamide (22). Yield 55.8%, yellow solid, m.p. 108–110 °C.^{1}H NMR (300 MHz, DMSO-d_6) δ: 10.68 (s, 1H), 8.42 (t, J = 6.3 Hz, 2H), 8.07–7.97 (m, 2H), 7.77–7.68 (m, 4H), 7.31 (d, J = 7.9 Hz, 4H), 6.72 (d, J = 9.0 Hz, 2H), 3.93 (s, 2H), 3.72 (s, 6H), 2.99 (s, 6H), 2.87 (s, 2H); ^{13}C NMR (75 MHz, DMSO-d_6) δ: 161.46, 159.96, 147.46, 147.10, 139.97, 137.10, 135.01, 133.63, 133.29, 129.93, 128.56, 128.12, 126.37, 125.15, 124.54, 123.14, 122.46, 122.25, 114.18, 111.68, 109.87, 58.5, 55.44, 54.05, 50.07, 32.43, 28.19; ESI-MS *m/z*: 579.6 [M + H]$^+$. Anal. Calcd for $C_{34}H_{31}FN_4O_4$: C, 70.57; H, 5.40; N, 9.68. Found: C, 70.56; H, 5.39; N, 9.67.

4.3.4.9. N-(4-(2-(6,7-dimethoxy-3,4-dihydroisoquinolin-2(1H)-yl)ethyl) phenyl)-3-(4-fluorophenyl)-4-oxo-3,4-dihydrophthalazine-1-carboxamide (23). Yield 69.2%, light yellow solid, m.p. 166–168 °C.^{1}H NMR (300 MHz, DMSO-d_6) δ: 10.60 (s, 1H), 8.41 (s, 2H), 8.09–7.94 (m, 2H), 7.83 (s, 2H), 7.68 (d, J = 6.9 Hz, 2H), 7.39 (t, J = 7.1 Hz, 2H), 7.28 (d, J = 6.9 Hz, 2H), 6.65 (d, J = 5.3 Hz, 2H), 3.70 (d, J = 1.2 Hz, 6H), 3.54 (s, 2H), 2.82 (s, 2H), 2.70 (s, 6H); ^{13}C NMR (75 MHz, DMSO-d_6) δ: 162.55, 161.37, 159.32, 158.16, 147.11, 146.87, 140.35, 137.52, 136.59, 136.07, 134.17, 132.62, 128.94, 128.32, 128.20, 127.88, 126.92, 126.82, 126.64, 126.37, 125.90, 120.24, 115.51, 115.20, 111.76, 109.96, 59.46, 55.43, 55.06, 50.52, 32.43, 28.29; ESI-MS *m/z*: 579.7 [M − H]$^+$. Anal. Calcd for $C_{34}H_{31}FN_4O_4$: C, 70.57; H, 5.40; N, 9.68. Found: C, 70.55; H, 5.41; N, 9.67.

4.3.4.10. 3-(2-bromophenyl)-N-(4-(2-(6,7-dimethoxy-3,4-dihydroisoquinolin-2(1H)-yl)ethyl)phenyl)-4-oxo-3,4-dihydrophthalazine-1-carboxamide (24). Yield 61.6%, yellow solid, m.p. 140–142 °C.^{1}H NMR (300 MHz, DMSO-d_6 δ:10.60 (s, 1H), 8.24 (d, J = 8.1 Hz, 2H), 7.98–7.92 (m, 2H), 7.71 (d, J = 6.8 Hz, 2H), 7.69–7.62 (m, 4H), 7.21 (d, J = 8.0 Hz, 2H), 6.67 (d, J = 9.0 Hz, 2H), 3.70 (s, 6H), 3.54 (s, 2H), 2.81 (s, 2H), 2.69 (s, 6H); ^{13}C NMR (75 MHz, DMSO-d_6) δ: 161.70, 158.67, 147.12, 146.87, 137.23, 137.02, 135.81, 133.09, 130.38, 129.52, 128.58, 128.35, 128.01, 126.58, 125.89, 123.03, 122.15, 121.11, 114.00, 111.69, 109.94, 59.44, 55.44, 55.06, 50.45, 32.46, 28.27; ESI-MS *m/z*: 639.6 [M + H]$^+$. Anal. Calcd for $C_{34}H_{31}BrN_4O_4$: C, 63.85; H, 4.89; N, 8.76. Found: C, 63.84; H, 4.88; N, 8.76.

4.3.4.11. 3-(3-bromophenyl)-N-(4-(2-(6,7-dimethoxy-3,4-dihydroisoquinolin-2(1H)-yl)ethyl)phenyl)-4-oxo-3,4-dihydrophthalazine-1-carboxamide (25). Yield 51.0%, yellow solid, m.p. 105–107 °C.^{1}H NMR (300 MHz, DMSO-d_6) δ:10.62 (s, 1H), 8.41 (t, J = 7.1 Hz, 3H), 8.12–7.96 (m, 4H), 7.67 (d, J = 8.4 Hz, 3H), 7.28 (d, J = 8.4 Hz, 2H), 6.65 (d, J = 6.5 Hz, 2H), 3.70 (d, J = 0.9 Hz, 6H), 3.54 (s, 2H), 2.81 (d, J = 7.1 Hz, 2H), 2.70 (s, 6H); ^{13}C NMR (75 MHz, DMSO-d_6) δ: 161.72, 159.46, 147.13, 146.89, 144.33, 136.83, 136.03, 133.31, 128.79, 128.64, 128.26, 126.63, 125.91, 123.49, 123.03, 122.23, 114.12, 111.75, 109.98, 59.49, 55.46, 55.09, 50.53, 32.54, 28.31; ESI-MS *m/z*: 639.5 [M + H]$^+$. Anal. Calcd for $C_{34}H_{31}BrN_4O_4$: C, 63.85; H, 4.89; N, 8.76. Found: C, 63.83; H, 4.88; N, 8.77.

4.3.4.12. 3-(4-chlorophenyl)-N-(4-(2-(6,7-dimethoxy-3,4-dihydroisoquinolin-2(1H)-yl)ethyl)phenyl)-4-oxo-3,4-dihydrophthalazine-1-carboxamide (26). Yield 62.8%, yellow solid, m.p.162–164 °C. ^{1}H NMR (300 MHz, DMSO-d_6) δ: 10.63 (s, 1H), 8.41 (t, J = 6.4 Hz, 2H), 8.19–7.93 (m, 2H), 7.85 (d, J = 8.2 Hz, 2H), 7.65 (dd, J = 18.7, 8.0 Hz, 4H), 7.27 (d, J = 7.6 Hz, 2H), 6.64 (d, J = 6.4 Hz, 2H), 3.70 (s, 6H), 3.54 (s, 2H), 2.82 (s, 2H), 2.69 (s, 6H); ^{13}C NMR (75 MHz, DMSO-d_6) δ: 161.33, 158.09, 147.10, 146.86, 140.56, 140.02, 136.60, 136.08, 134.24, 132.67, 132.19, 128.94, 128.53, 127.79, 126.86, 126.63, 126.39, 125.90, 120.24, 111.76, 109.96, 59.47, 55.46, 55.06, 50.52, 32.44, 28.29; ESI-MS *m/z*: 595.6 [M + H]$^+$. Anal. Calcd for $C_{34}H_{31}ClN_4O_4$: C, 68.62; H, 5.25; N, 9.41. Found: C, 68.63; H, 5.24; N, 9.41.

4.3.4.13. N-(4-(2-(6,7-dimethoxy-3,4-dihydroisoquinolin-2(1H)-yl)ethyl) phenyl)-3-(4-nitrophenyl)-4-oxo-3,4-dihydrophthalazine-1-carboxamide (27). Yield 53.9%, yellow solid, m.p.183–185 °C. ^{1}H NMR (300 MHz, DMSO-d_6) δ: 10.69 (s, 1H), 8.54–8.26 (m, 4H), 8.18 (d, J = 8.7 Hz, 2H), 8.07–7.82 (m, 2H), 7.69 (d, J = 8.1 Hz, 2H), 7.29 (d, J = 8.0 Hz, 2H), 6.65 (d, J = 6.4 Hz, 2H), 3.70 (s, 6H), 3.54 (s, 2H), 2.80 (s, 2H), 2.70 (s, 6H); ^{13}C NMR (75 MHz, DMSO-d_6) δ: 161.17, 158.21, 146.89, 146.22, 141.21, 136.71, 135.99, 134.50, 132.88, 128.94, 127.85, 126.83, 125.93, 123.92, 120.29, 111.81, 110.02, 59.37, 55.50, 55.04, 50.49, 32.41, 28.25; ESI-MS *m/z*: 606.6 [M + H]$^+$. Anal. Calcd for $C_{34}H_{31}N_5O_6$: C, 67.43; H, 5.16; N, 11.56. Found: C, 67.44; H, 5.16; N, 11.55.

4.3.4.14. 3-(4-cyanophenyl)-N-(4-(2-(6,7-dimethoxy-3,4-dihydroisoquinolin-2(1H)-yl)ethyl)phenyl)-4-oxo-3,4-dihydrophthalazine-1-carboxamide (28). Yield 68.3%, yellow solid, m.p.165–167 °C. ^{1}H NMR (300 MHz, DMSO-d_6) δ: 10.64 (s, 1H), 8.43 (t, J = 6.2 Hz, 3H), 8.06 (d, J = 7.6 Hz, 4H), 7.67 (d, J = 7.0 Hz, 2H), 7.28 (d, J = 7.6 Hz, 2H), 6.65 (d, J = 6.3 Hz, 2H), 3.70 (s, 6H), 3.56 (s, 2H), 2.83–2.71 (m, 8H); ^{13}C NMR (75 MHz, DMSO-d_6) δ: 161.87, 158.10, 147.13, 146.87, 137.11, 135.69, 134.85, 132.98, 130.03, 128.54, 127.93, 126.50, 125.85, 125.68, 123.06, 122.15, 121.08, 115.24, 114.95, 113.91, 111.66, 109.90, 59.36, 55.41, 54.99, 50.36, 32.40, 28.21; ESI-MS *m/z*: 586.6 [M + H]$^+$. Anal. Calcd for $C_{35}H_{31}N_5O_4$: C, 71.78; H, 5.34; N, 11.96. Found: C, 71.77; H, 5.33; N, 11.96.

4.3.4.15. N-(4-(2-(6,7-dimethoxy-3,4-dihydroisoquinolin-2(1H)-yl)ethyl) phenyl)-3-(3,4-dimethylphenyl)-4-oxo-3,4-dihydrophthalazine-1-carboxamide (29). Yield 60.7%, yellow solid, m.p.133–135 °C. ^{1}H NMR (300 MHz, DMSO-d_6) δ: 10.56 (s, 1H), 8.39 (s, 2H), 7.99 (s, 2H), 7.67 (d, J = 7.4 Hz, 2H), 7.55–7.40 (m, 2H), 7.28 (s, 3H), 6.64 (d, J = 6.3 Hz, 2H), 3.69 (s, 6H), 3.54 (s, 2H), 2.79–2.69 (m, 8H), 2.29 (s, 6H); ^{13}C NMR (75 MHz, DMSO-d_6) δ: 161.54, 158.38, 147.13, 146.89, 139.85, 137.20, 135.70, 132.99, 128.96, 128.58, 127.88, 126.67, 125.93, 125.55, 122.96, 122.00, 113.94, 111.76, 109.99, 59.49, 55.43, 55.10, 50.50, 32.48, 28.31, 20.96, 19.91; ESI-MS *m/z*: 589.6 [M + H]$^+$. Anal. Calcd for $C_{36}H_{36}N_4O_4$: C, 73.45; H, 6.16; N, 9.52. Found: C, 73.44; H, 6.16; N, 9.54.

4.3.4.16. 3-(2,6-difluorophenyl)-N-(4-(2-(6,7-dimethoxy-3,4-dihydroisoquinolin-2(1H)-yl)ethyl)phenyl)-4-oxo-3,4-dihydrophthalazine-1-carboxamide (30). Yield 62.7%, yellow solid, m.p. 166–168 °C. ^{1}H NMR (300 MHz, DMSO-d_6) δ: 10.62 (s, 1H), 8.41 (d, J = 7.4 Hz, 2H), 8.06 (d, J = 9.0 Hz, 2H), 7.78–7.50 (m, 5H), 7.29 (s, 2H), 6.64 (d, J = 6.3 Hz, 2H), 3.70 (s, 6H), 3.55 (s, 2H), 2.81–2.70 (m, 8H); ^{13}C NMR (75 MHz, DMSO-d_6) δ: 162.18, 159.64, 147.11, 146.86, 137.98 (s), 137.68, 136.84, 136.01, 130.48, 128.60, 128.33, 128.02, 126.70, 126.63, 125.98, 125.90, 125.23, 122.15, 112.67, 111.72, 109.95, 59.45, 55.41, 55.08, 50.47, 32.47, 28.30; ESI-MS *m/z*: 597.6 [M + H]$^+$. Anal. Calcd for $C_{34}H_{30}F_2N_4O_4$: C, 68.45; H, 5.07; N, 9.39. Found: C, 68.44; H, 5.06; N, 9.39.

4.3.4.17. 3-(3,4-dichlorophenyl)-N-(4-(2-(6,7-dimethoxy-3,4-dihydroisoquinolin-2(1H)-yl)ethyl)phenyl)-4-oxo-3,4-dihydrophthalazine-1-carboxamide (31). Yield 46.7%, yellow solid, m.p. 147–149 °C. ^{1}H NMR (300 MHz, DMSO-d_6) δ: 10.77 (s, 1H), 8.42 (d, J = 7.6 Hz, 2H), 8.11–7.93 (m, 3H), 7.89–7.79 (m, 2H), 7.69 (d, J = 8.3 Hz, 2H), 7.28 (d, J = 8.2 Hz, 2H), 6.65 (d, J = 6.3 Hz, 2H), 3.70 (s, 6H), 3.54 (s, 2H), 2.81 (d, J = 7.4 Hz, 2H), 2.70 (s, 6H); ^{13}C NMR (75 MHz, DMSO-d_6) δ: 161.23, 158.10, 147.11, 146.86, 140.79, 140.71, 136.62, 136.08, 134.32, 132.73, 130.88, 130.38, 128.92, 127.85, 127.80, 126.85, 126.64, 126.48, 126.25, 125.90, 120.33, 111.76, 109.97, 59.43, 55.47, 55.05, 50.50, 32.43, 28.27; ESI-MS m/z: 629.6 $[M+H]^+$. Anal. Calcd for $C_{34}H_{30}Cl_2N_4O_4$: C, 64.87; H, 4.80; N, 8.90. Found: C, 64.88; H, 4.81; N, 8.92.

4.3.4.18. 3-(3,5-bis(trifluoromethyl)phenyl)-N-(4-(2-(6,7-dimethoxy-3,4-dihydroisoquinolin-2(1H)-yl)ethyl)phenyl)-4-oxo-3,4-dihydrophthalazine-1-carboxamide (32). Yield 58.1%, yellow solid, m.p. 118–120 °C.^{1}H NMR (300 MHz, DMSO-d_6) δ: 10.73 (s, 1H), 8.63 (s, 2H), 8.44 (d, J = 5.1 Hz, 2H), 8.23 (s, 1H), 8.13–7.89 (m, 2H), 7.69 (d, J = 7.8 Hz, 2H), 7.29 (d, J = 7.4 Hz, 2H), 6.64 (d, J = 5.5 Hz, 2H), 3.70 (s, 6H), 3.54 (s, 2H), 2.82 (d, J = 7.4 Hz, 2H), 2.70 (s, 6H); ^{13}C NMR (75 MHz, DMSO-d_6) δ: 161.95, 158.77, 147.12, 146.88, 137.18, 135.80, 132.99, 130.94, 128.47, 127.87, 126.64, 125.91, 125.32, 122.94, 122.27, 120.93, 113.71, 111.76, 111.28, 110.98, 109.97, 59.64, 55.46, 55.1, 50.56, 32.47, 28.29; ESI-MS m/z: 697.6 $[M+H]^+$. Anal. Calcd for $C_{36}H_{30}F_6N_4O_4$: C, 62.07; H, 4.34; N, 8.04. Found: C, 62.06; H, 4.33; N, 8.03.

4.3.4.19. N-(4-(2-(6,7-dimethoxy-3,4-dihydroisoquinolin-2(1H)-yl)ethyl)phenyl)-4-oxo-3-(pyridin-2-yl)-3,4-dihydrophthalazine-1-carboxamide (33). Yield 58.1%, yellow solid, m.p. 147–149 °C.^{1}H NMR (300 MHz, DMSO-d_6) δ: 10.68 (s, 1H), 8.67 (s, 1H), 8.37 (dd, J = 7.2, 3.0 Hz 2H), 8.06–8.02 (m, 4H), 7.78–7.58 (m, 3H), 7.27 (d, J = 6.9 Hz, 2H), 6.67 (d, J = 7.0 Hz, 2H), 3.71 (s, 6H), 3.59 (s, 2H), 2.88 (d, J = 8.8 Hz, 2H), 2.71 (s, 6H); ^{13}C NMR (75 MHz, DMSO-d_6) δ:161.86, 158.08, 147.12, 146.88, 145.55, 136.83, 136.11, 133.35, 128.65, 128.29, 126.66, 125.92, 123.08, 122.29, 121.73, 114.42, 111.77, 109.99, 59.48, 55.47, 55.09, 50.52, 32.49, 28.31; ESI-MS m/z: 562.6 $[M+H]^+$. Anal. Calcd for $C_{33}H_{31}N_5O_4$: C, 70.57; H, 5.56; N, 12.47. Found: C, 70.56; H, 5.55; N, 12.47.

Conflicts of interest

The authors declare no conflict of interest.

Acknowledgements

This study was supported by National Natural Science Foundation of China (No. 81872733 and 81803353)

References

[1] M.M. Gottesman, Mechanisms of cancer drug resistance, Annu. Rev. Med. 53 (2002) 615–627.
[2] S.K. Nigam, What do drug transporters really do? Nat. Rev. Drug Discov. 14 (2015) 29–44.
[3] Z. Chen, T. Shi, L. Zhang, P. Zhu, M. Deng, C. Huang, T. Hu, L. Jiang, J. Li, Mammalian drug efflux transporters of the ATP binding cassette (ABC) family in multidrug resistance: a review of the past decade, Cancer Lett. 370 (2016) 153–164.
[4] K.P. Locher, Review structure and mechanism of ATP-binding cassette transporters, Philos. Trans. R Soc. Lond. B Biol. Sci. 364 (2009) 239–245.
[5] B. Sarkadi, L. Homolya, G. Szakacs, A. Varadi, Human multidrug resistance ABCB and ABCG transporters: participation in a chemoimmunity defense system, Physiol. Rev. 86 (2006) 1179–1236.
[6] J.I. Fletcher, R.T. Williams, M.J. Henderson, M.D. Norris, M. Haber, ABC transporters as mediators of drug resistance and contributors to cancer cell biology, Drug Resist. Updat. 26 (2016) 1–9.
[7] F.J. Sharom, ABC multidrug transporters: structure, function and role in chemoresistance, Pharmacogenomics 9 (2008) 105–127.
[8] A. Palmeira, E. Sousa, M.H. Vasconcelos, M.M. Pinto, Three decades of P-gp inhibitors: skimming through several generations and scaffolds, Curr. Med. Chem. 19 (2012) 1946–2025.
[9] T. Tsuruo, H. Iida, S. Tsukagoshi, Y. Sakurai, Overcoming of vincristine resistance in P388 leukemia in vivo and in vitro through enhanced cytotoxicity of vincristine and vinblastine by verapamil, Cancer Res. 41 (1981) 1967–1972.
[10] R. Krishna, L.D. Mayer, Multidrug resistance (MDR) in cancer Mechanisms, reversal using modulators of MDR and the role of MDR modulators in influencing the pharmacokinetics of anticancer drugs, Eur. J. Pharm. Sci. 11 (2000) 265–283.
[11] D.R. Ferry, H. Traunecker, D.J. Kerr, Clinical trials of P-glycoprotein reversal in solid tumours, Eur. J. Cancer 32A (1996) 1070–1081.
[12] Y.J. Mi, Y.J. Liang, H.B. Huang, H.Y. Zhao, C.P. Wu, F. Wang, L.Y. Tao, C.Z. Zhang, C.L. Dai, A.K. Tiwari, X.X. Ma, K.K. To, S.V. Ambudkar, Z.S. Chen, L.W. Fu, Apatinib (YN968D1) reverses multidrug resistance by inhibiting the efflux function of multiple ATP-binding cassette transporters, Cancer Res. 70 (2010) 7981–7991.
[13] Y.J. Wang, R.J. Kathawala, Y.K. Zhang, A. Patel, P. Kumar, S. Shukla, K.L. Fung, S.V. Ambudkar, T.T. Talele, Z.S. Chen, Motesanib (AMG706), a potent multikinase inhibitor, antagonizes multidrug resistance by inhibiting the efflux activity of the ABCB1, Biochem. Pharmacol. 90 (2014) 367–378.
[14] Q. Qiu, B. Liu, J. Cui, Z. Li, X. Deng, H. Qiang, J. Li, C. Liao, B. Zhang, W. Shi, M. Pan, W. Huang, H. Qian, Design, synthesis, and pharmacological characterization of N-(4-(2 (6,7-dimethoxy-3,4-dihydroisoquinolin-2(1H)yl)ethyl)phenyl)quinazolin-4-amine derivatives: novel inhibitors reversing P-glycoprotein-mediated multidrug resistance, J. Med. Chem. 60 (2017) 3289–3302.
[15] Z. Liu, R. Wang, R. Guo, J. Hu, R. Li, Y. Zhao, P. Gong, Design, synthesis and biological evaluation of novel 6,7-disubstituted-4-phenoxyquinoline derivatives bearing 4-oxo-3,4-dihydrophthalazine-1-carboxamide moieties as c-Met kinase inhibitors, Bioorg. Med. Chem. 22 (2014) 3642–3653.
[16] K.F. Chan, I.L. Wong, J.W. Kan, C.S. Yan, L.M. Chow, T.H. Chan, Amine linked flavonoid dimers as modulators for P-glycoprotein-based multidrug resistance: structure-activity relationship and mechanism of modulation, J. Med. Chem. 55 (2012) 1999–2014.
[17] S.A. Jabbar, P.R. Twentyman, J.V. Watson, The MTT assay underestimates the growth inhibitory effects of interferons, Br. J. Cancer 60 (1989) 523–528.
[18] L.W. Fu, Y.M. Zhang, Y.J. Liang, X.P. Yang, Q.C. Pan, The multidrug resistance of tumour cells was reversed by tetrandrine in vitro and in xenografts derived from human breast adenocarcinoma MCF-7/adr cells, Eur. J. Cancer 38 (2002) 418–426.
[19] N.N. Wang, L.J. Zhao, L.N. Wu, M.F. He, J.W. Qu, Y.B. Zhao, W.Z. Zhao, J.S. Li, J.H. Wang, Mechanistic analysis of taxol-induced multidrug resistance in an ovarian cancer cell line, Asian Pac. J. Cancer Prev. 14 (2013) 4983–4988.
[20] J.M. Sargent, C.G. Taylor, Appraisal of the MTT assay as a rapid test of chemosensitivity in acute myeloid leukaemia, Br. J. Cancer 60 (1989) 206–210.
[21] I.L. Wong, K.F. Chan, K.H. Tsang, C.Y. Lam, Y. Zhao, T.H. Chan, L.M. Chow, Modulation of multidrug resistance protein 1 (MRP1/ABCC1)-mediated multidrug resistance by bivalent apigenin homodimers and their derivatives, J. Med. Chem. 52 (2009) 5311–5322.